

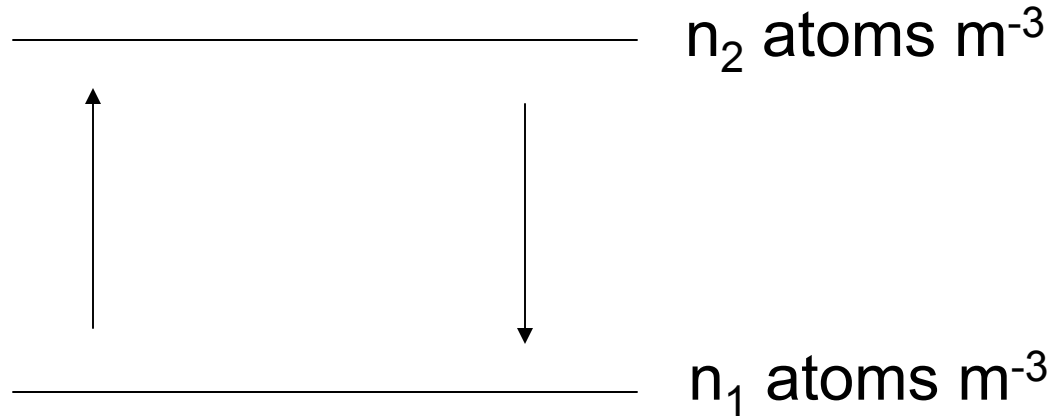
Components of Galaxies – Gas

The Importance of Gas

- Fuel for star formation (H_2)
- Tracer of galaxy kinematics/mass (HI)
- Tracer of dynamical history of interaction between galaxies (HI)

The Two-Level Atom

Consider an atom comprised of only two levels, 1 & 2



When the atoms jumps from 2 to 1, it emits a photon of frequency ν_{21} & energy $h\nu_{21}$, where h is the Planck constant (6.63×10^{-34} J·s).

Spontaneous Transition Probability

from 2 to 1 is expressed in terms of the Einstein coefficient A_{21} (s^{-1} per atom). The energy released per second per cubic meter through spontaneous decay is thus

$$h\nu_{21}A_{21}n_2 \text{ (W m}^{-3}\text{)}.$$

Stimulated Transition Probability

is expressed in terms of the Einstein coefficient B_{21} & the energy density U_{21} ($= I_\nu / c$) such that the energy released per second per cubic meter per atom is,

$$B_{21}U_{21} \text{ (W m}^{-3} \text{ atom}^{-1}\text{)}.$$

Similarly, B_{12} represents the stimulated up transition probability.

The net number of absorptions per unit volume per second is then

$$(n_1 B_{12} - n_2 B_{21}) U_{21} \text{ (W m}^{-3}\text{)},$$

And thus the energy absorbed per unit volume per second is,

$$(n_1 B_{12} - n_2 B_{21}) U_{21} h\nu_{21} = \int \kappa_\nu I_\nu d\nu \text{ (W m}^{-3} \text{ s}^{-1}\text{)},$$

Where κ_ν is the absorption coefficient. Note that the source Function, S , is simply the ratio of the emission coefficient & the absorption coefficient j_ν ,

$$S = \frac{j_\nu}{\kappa_\nu}.$$

Given,

$$(n_1 B_{12} - n_2 B_{21}) U_{21} h\nu_{21} = \int \kappa_\nu I_\nu d\nu \quad (\text{W m}^{-3} \text{ s}^{-1}),$$

I_ν / c can be substituted for U_{21} to get

$$\int \kappa_\nu d\nu = (n_1 B_{12} - n_2 B_{21}) \frac{h\nu_{21}}{c}.$$

Balancing the absorption rate with the emission rate,

$$\int j_\nu d\nu = I_\nu \int \kappa_\nu d\nu,$$

In terms of Einstein coefficients,

$$\frac{h\nu_{21} n_2}{4\pi} = (n_1 B_{12} - n_2 B_{21}) \frac{I_\nu}{c},$$

where the factor 4π comes from integrating over 4π steradian solid angle.

Rearranging the terms in

$$A_{21} \frac{h\nu_{21} n_2}{4\pi} = (n_1 B_{12} - n_2 B_{21}) \frac{I_\nu}{c},$$

And solving for I_ν ,

$$I_\nu = \frac{(A_{21}/B_{21})c}{4\pi \left(\frac{n_1 B_{12}}{n_2 B_{21}} - 1 \right)}.$$

In **Thermodynamic equilibrium**,

$$B_\nu = \frac{2h\nu^3}{c^2} \frac{1}{e^{h\nu/kT} - 1}.$$

Thus, given that the levels are populated as

$$\frac{n_2}{n_1} = \frac{g_2}{g_1} e^{-h\nu/kT},$$

where g_1 & g_2 are statistical weights & T is the excitation temperature,

The Einstein coefficients are equal to.

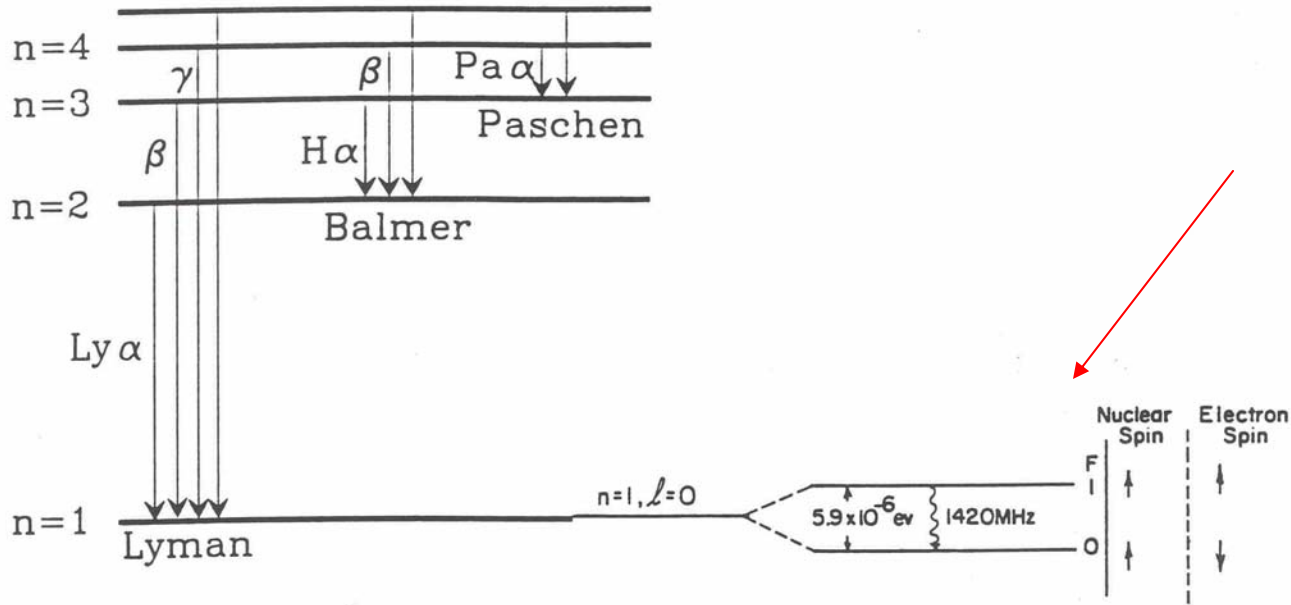
$$\frac{A_{21}}{B_{21}} = \frac{8\pi h\nu^3}{c^3},$$

$$B_{12}g_1 = B_{21}g_2.$$

Table 1. Phases of the ISM

Phase	Acronym	State of H	Approx Kinetic Temp. (K)	Approx Density n (cm^{-3})	Exponential Scale Height (pc)	Mass (M_{\odot})
Molecular Gas	MNM	H ₂	15	>300	60	2.5×10^9
Cold HI	CNM	HI	80	40	130	2.5×10^9
Warm HI	WNM	HI	8000	0.4	350	1×10^8
HII Regions	WIM	HII	8000	$\gtrsim 1$	750	1×10^8
Coronal Gas	HIM	HII	10^6	0.003	3000	$\sim 1 \times 10^6$

Neutral Hydrogen



Energy level diagram for the *hyperfine splitting* of the ground state of the hydrogen atom. The state in which the electron and proton spins are aligned has a slightly higher energy.

- A source of strong emission in galaxies is the 21 cm neutral hydrogen emission line.
- The line arises from the **flip** in the **spin state** of an electron in the ground state of neutral hydrogen.

Neutral Hydrogen, cont.

- Forbidden transition, with $A_{10} = 2.9 \times 10^{-15} \text{ s}^{-1}$.
- Transition rate lifetime is $t_{10} = 1.1 \times 10^7$ years
- Why is the signal strong? High HI column density (i.e., $N_{\text{HI}} = 10^{21} \text{ cm}^{-2}$).
- I.e., if $n_1 \ell$ is large, where ℓ is the length along the line of sight containing HI, then $h \nu_{10} n_1 \ell$ is large.

In galaxies, collisions dominate 21 cm transitions

- I.e., emitting clouds are in thermodynamic equilibrium.

Determination of collision time:

- 1) collisional cross section $\sigma = \pi (2 \times 10^{-8} \text{ cm})^2 = 1 \times 10^{-15} \text{ cm}^2$
- 2) atomic density $N = 1 \text{ cm}^{-3}$

The mean free path is

$$l = \frac{1}{N\sigma} = 1 \times 10^{15} \text{ cm.}$$

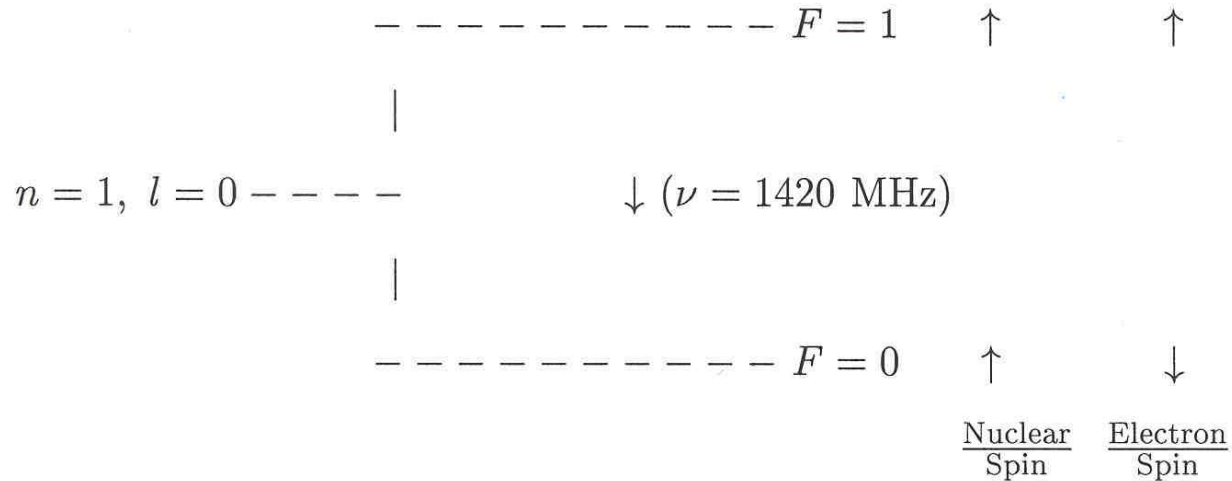
Atomic gas in galaxies has $T = 100\text{K}$, thus the velocity v is,

$$v = \left(\frac{3kT}{m} \right)^{1/2} = 1.6 \times 10^5 \text{ cm s}^{-1}.$$

Thus, the time between collisions is

$$t_{\text{collision}} = \frac{l}{v} \approx 200 \text{ years.}$$

- Most of the electrons in neutral hydrogen are in the F=1 state.



- This can be shown by comparing

$$\Delta E = h \nu / k \quad \leftrightarrow \quad T_{\text{ex}} = 100 \text{ K (Typical HI } T)$$

Thus,

$$\frac{n_1}{n_0} = \frac{g_1}{g_0} e^{-h\nu/kT_{\text{ex}}} \sim 3,$$

where $g_F = 2F + 1$. Since $n_1 \sim 3n_0$,
 then $n_{\text{HI}} = n_1 + n_0 = 4n_0$

Optical Depth

- For HI at $T = 100$ K, $h\nu \ll kT$.
- Thus, the spin states are populated

$$\frac{n_1}{n_0} = 3e^{-h\nu/kT_{\text{ex}}} = 3 \left(1 - \frac{h\nu}{kT_{\text{ex}}} \right),$$

where $g_1 / g_0 = 3$. Similarly,

$$B_{01} = 3B_{10}.$$

HI absorption occurring from transitions are proportional to

$$n_0 B_{01} - n_1 B_{10} = n_0 B_{01} - 3n_0 \left(1 - \frac{h\nu}{kT} \right) \frac{B_{01}}{3} = n_0 B_{01} \frac{h\nu}{kT_{\text{ex}}},$$

Making the substitution $n_0 = \frac{1}{4} n_{\text{H}}$

$$\propto n_{\text{H}} B_{01} \frac{h\nu}{4kT_{\text{ex}}}.$$

The optical depth, τ , is thus,

$$\tau(\nu) = N_H f(\nu) B_{01} \frac{h\nu}{4kT} = 5.489 \times 10^{-20} \frac{n_H}{T_{\text{ex}}} f(\nu),$$

Where

1) N_H = H column density

2) $f(\nu)$ is a function that accounts for the contribution of 21 cm emission occurring at velocity ν .

$f(\nu)$ is normalized such that,

$$\int_{-\infty}^{\infty} f(\nu) d\nu = 1.$$

A useful form is

$$f(\nu) = \frac{1}{\pi^{1/2} b} e^{-(\Delta\nu/b)^2},$$

where

$$b = (2kT/m)^{1/2}.$$

Hydrogen Column Density

The above expression can be rewritten & solved for hydrogen column density

$$N_H = 1.82 \times 10^{22} \int_{-\infty}^{\infty} T\tau(\nu) d\nu \text{ [atoms m}^{-2}\text{]}$$

Or for $\tau \ll 1$,

$$N_H = 1.82 \times 10^{22} \int_{-\infty}^{\infty} T_B d\nu \text{ [atoms m}^{-2}\text{]}.$$

In terms of HI Mass,

$$M_{\text{HI}} = 2.356 \times 10^5 d^2 \int_{-\infty}^{\infty} S(v) dv,$$

where,

- 1) d is in units of Mpc
- 2) $S(v) dv$ is in units of Jy km s⁻¹.

HI in Emission & Absorption

HI is seen in both emission & absorption, depending on the optical depth & presence of background continuum source.

Consider the equation of radiative transfer,

$$\frac{\partial I_\nu}{\partial \tau_\nu} = I_\nu - S_\nu.$$

Multiplying through by $e^{-\tau_\nu}$ & rearranging the terms,

$$e^{-\tau_\nu} \frac{\partial I_\nu}{\partial \tau_\nu} + e^{-\tau_\nu} I_\nu = e^{-\tau_\nu} S_\nu,$$

$$\frac{\partial I_\nu e^{-\tau_\nu}}{\partial \tau_\nu} = e^{-\tau_\nu} S_\nu.$$

For an isothermal cloud in **LTE**, $S_\nu = B_\nu = \text{constant}$.
Integrating yields,

$$I_\nu(\tau_\nu) = I_\nu(0)e^{-\tau_\nu} + (1 - e^{-\tau_\nu})S_\nu.$$

For this equation,

- 1) $I_\nu(0)$ is the intensity of the background source
- 2) S_ν is the intensity generated within the cloud.

Typically, radio astronomers use temperatures instead of fluxes, where temperature is simply that given by the Planck function in the Rayleigh-Jean regime.

Thus, for I_ν & S_ν ,

$$I_\nu = \frac{2kT_B\nu^2}{c^2} \quad \text{and} \quad S_\nu = \frac{2kT_{\text{cloud}}\nu^2}{c^2},$$

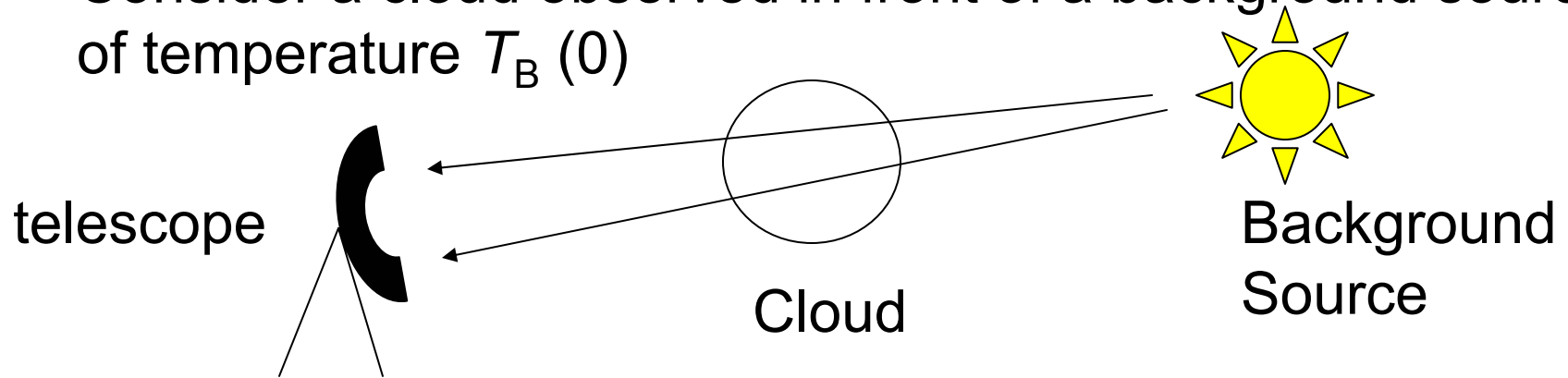
where $T_B = \text{brightness temperature}$ & $T_{\text{cloud}} = \text{cloud temperature}$

Thus,

$$I_\nu(\tau_\nu) = I_\nu(0)e^{-\tau_\nu} + (1 - e^{-\tau_\nu})S_\nu.$$

$$T_B(\tau_\nu) = T_B(0)e^{-\tau_\nu} + (1 - e^{-\tau_\nu})T_{\text{cloud}}.$$

- How does the temperature measured change with τ ?
Consider a cloud observed in front of a background source of temperature $T_B(0)$



For $\tau \rightarrow 0$, $T_B \rightarrow T_B(0)(1 - \tau) + T_{\text{cloud}}\tau \rightarrow T_B(0)$.

and

for $\tau \rightarrow \infty$, $T_B \rightarrow T_{\text{cloud}}$.

Molecular Gas

- Molecular hydrogen clouds are the sites of star formation
- Dust grain surfaces are the catalyst for H₂ formation
- The ratio of the number densities of dust grains to hydrogen atoms is $n_g / n_H = 10^{-12}$.
- The formation rate of H₂ is thus,

$$\frac{dn_{\text{H}_2}}{dt} = \frac{1}{2}n_H(\pi a_g^2)n_g v_H \text{ [m}^{-3}\text{s}^{-1}\text{]},$$

where πa^2 is the grain cross section ($a = 1 \times 10^{-7}$ m) and

$$v_H = (3kT/2\mu m_H)^{1/2}.$$

For gas at a temperature of 100 K, $v_H = 1000$ m s⁻¹. Thus,

$$\frac{dn_{\text{H}_2}}{dt} = 1.5 \times 10^{-23} n_H^2 \text{ [m}^{-3}\text{ s}^{-1}\text{]}.$$

- The destruction rate of H_2 is 10^{-10} s^{-1} . Specifically,
 - 1) 10^{-10} s^{-1} for $N_{H_2} < 10^{18} \text{ m}^{-2}$
 - 2) & 10^{-14} s^{-1} for $N_{H_2} = 10^{24} \text{ m}^{-2}$.
- Thus, the destruction rate is equal to the formation rate when,

$$10^{-10} n_{H_2} [\text{m}^{-3} \text{ s}^{-1}] = 1.5 \times 10^{-23} n_H^2 [\text{m}^{-3} \text{ s}^{-1}]$$

$$n_{H_2} [\text{m}^{-3}] = 1.5 \times 10^{-13} n_H^2 [\text{m}^{-3}].$$

The cross section for photodissociation is $\sigma_{PD} = 10^{-18} \text{ m}^2$. Thus,

$$n_{H_2} l = \frac{1}{\sigma_{PD}} = 10^{18} [\text{m}^{-2}].$$

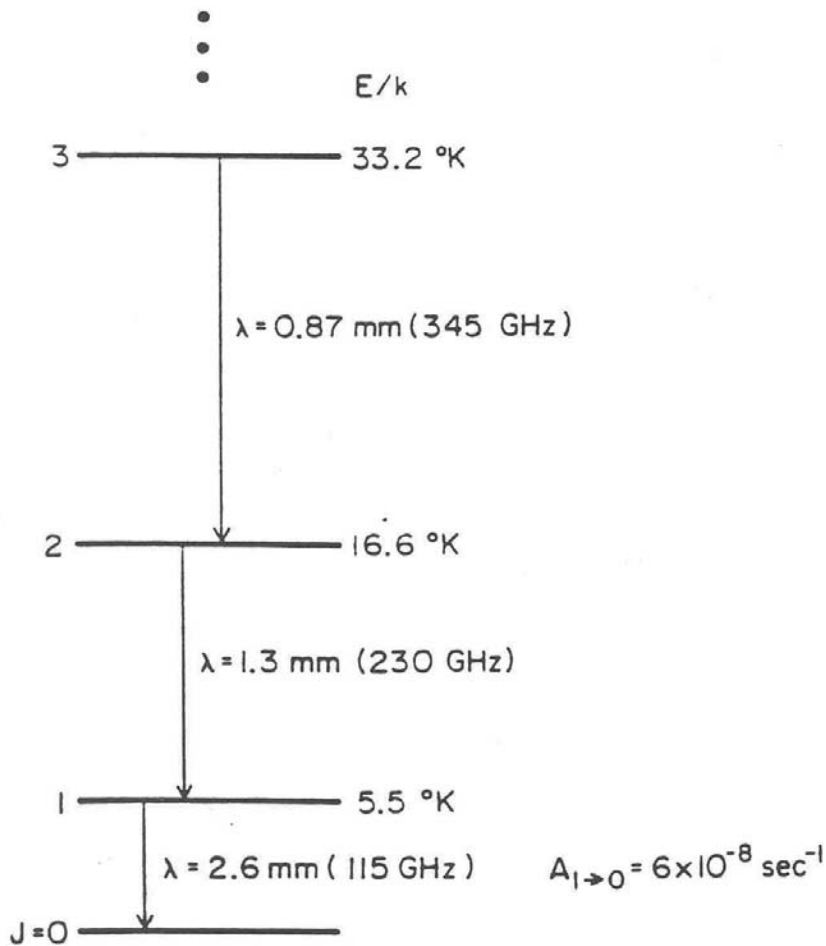
where l is the path length.

Thus, the condition required for significant shielding of dissociating radiation is,

$$1.5 \times 10^{-13} n_H^2 l \text{ [m}^{-2}\text{]} \gg 10^{18} \text{ [m}^{-2}\text{]}.$$

Thus, for a cloud with moderate hydrogen number density of $n_H \sim 10^8 \text{ m}^{-3}$, the core can be molecular if the shell thickness is on the order of $l \sim 1 \text{ pc}$.

CO as a Tracer of Molecular Hydrogen



- H_2 has no easily observed transitions
- $28 \mu\text{m} \rightarrow$ from space
- $2 \ \& \ 12 \mu\text{m} \rightarrow$ only warm ($T=100\text{K}$) H_2
- $\text{CO} \rightarrow$ collisionally excited by H_2 .

Collisional Excitation of CO

- The collisional coefficient is given by

$$C = v_{\text{H}_2} \sigma_{\text{CO}} N_{\text{CO}},$$

where

- 1) v_{H_2} is the velocity of H_2 molecules
 - 2) σ_{CO} is the collisional cross section of CO
 - 3) N_{CO} is the number density of CO
- For significant emission from collisions, $C = A_{J,J-1}$, where $A_{J,J-1}$ is the Einstein coefficient for spontaneous emission. Thus,

$$N_{\text{crit}} = \frac{A_{J,J-1}}{v_{\text{H}_2} \sigma_{\text{CO}}}.$$

The CO lines are optically thick, $\tau \gg 1$, thus N_{crit} must be divided by the number of steps, N_{esc} , it takes for a photon to random walk out of the molecular cloud,

$$N_{\text{crit}} = \frac{A_{J,J-1}}{N_{\text{esc}} v_{\text{H}_2} \sigma_{\text{CO}}}.$$

- Thus, for CO(1→0), $N_{\text{crit}} > 3000 \text{ cm}^{-3}$ (for $\tau \ll 1$), and few 100 cm^{-3} (for $\tau \gg 1$).

The Mass of Molecular Hydrogen Clouds

- CO luminosity can be used to calculate the H₂ mass.

The CO luminosity, L_{CO} , of a molecular cloud is,

$$L_{\text{CO}} = \pi R^2 T_{\text{CO}} \Delta v,$$

where,

1) R = radius of the cloud

2) $T_{\text{CO}} \Delta v$ = flux of the CO emission line

- For a cloud in **virial equilibrium**, twice the time averaged kinetic energy KE is equal to the negative of the time-averaged potential energy W

$$2KE = -W \quad \rightarrow \quad \Delta v^2 = \frac{GM_{\text{cloud}}}{R}$$

Substituting in for Δv in the luminosity equation,

$$L_{\text{CO}} = \pi R^2 T_{\text{CO}} \left(\frac{GM_{\text{cloud}}}{R} \right)^{1/2} = \pi T_{\text{CO}} (GM_{\text{cloud}})^{1/2} R^{3/2}.$$

Because,

$$R^3 = \left(\frac{3M_{\text{cloud}}}{4\pi\rho} \right),$$

then,

$$L_{\text{CO}} = \pi T_{\text{CO}} (GM_{\text{cloud}})^{1/2} \left(\frac{3M_{\text{cloud}}}{4\pi\rho} \right)^{1/2} = T_{\text{CO}} \left(\frac{3\pi G}{4\rho} \right)^{1/2} M_{\text{cloud}}.$$

Solving for M_{cloud} yields,

$$M_{\text{cloud}} = L_{\text{CO}} \left(\frac{4\rho}{3\pi G} \right)^{1/2} \frac{1}{T_{\text{CO}}}.$$

It turns out that

$$\frac{\rho^{1/2}}{T_{\text{CO}}} \approx \text{constant},$$

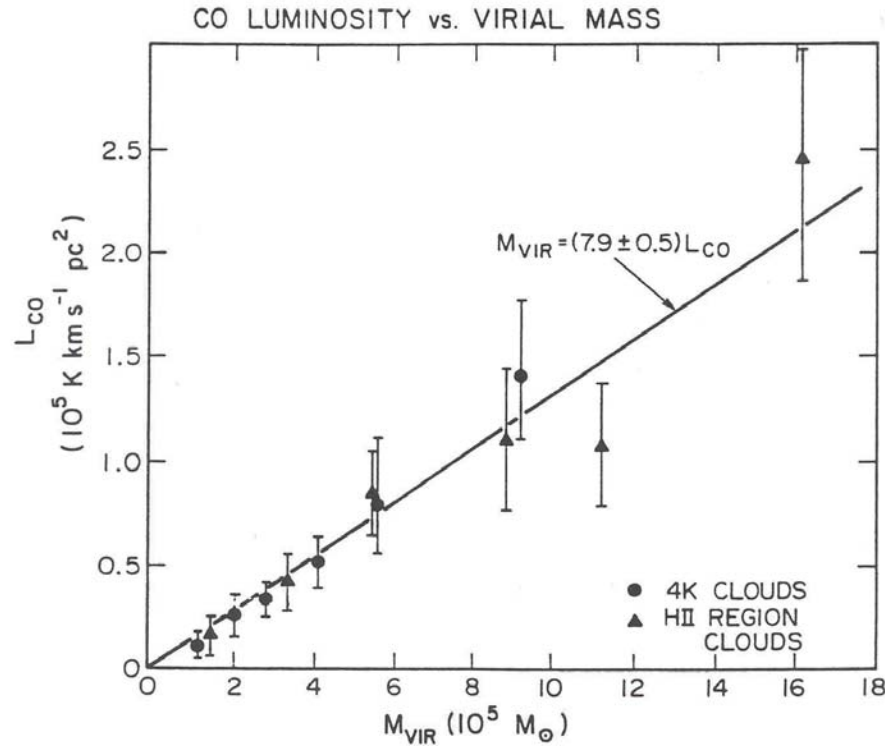
i.e., high density clouds are hot, low density clouds are cold.

Thus,

$$M_{\text{cloud}} \propto L_{\text{CO}}.$$

The proportionality constant is α .

What is α ?



(Scoville & Sanders, in Inter-Stellar Processes)

Figure 2. The CO luminosity is closely correlated with the virial masses of the clouds both with and without massive OB star formation (Scoville *et al* 1986). This linear proportionality justifies the use of CO as a tracer of the galactic H₂ mass. The best fit is equivalent to a constant of proportionality of $3.6 \times 10^{20} \text{ H}_2 \text{ cm}^{-2} (\text{K km s}^{-1})^{-1}$.

- L_{CO} vs. dynamical mass in molecular clouds
- So, $\alpha = 4 M_{\text{solar}} (\text{K km s}^{-1} \text{ pc}^2)^{-1}$
- Note the scatter!

Dynamical Mass Determinations

In external galaxies, the virial theorem can be used to calculate the dynamical mass of a CO disk, & thus determine an upper limit on α .

Dynamical mass is

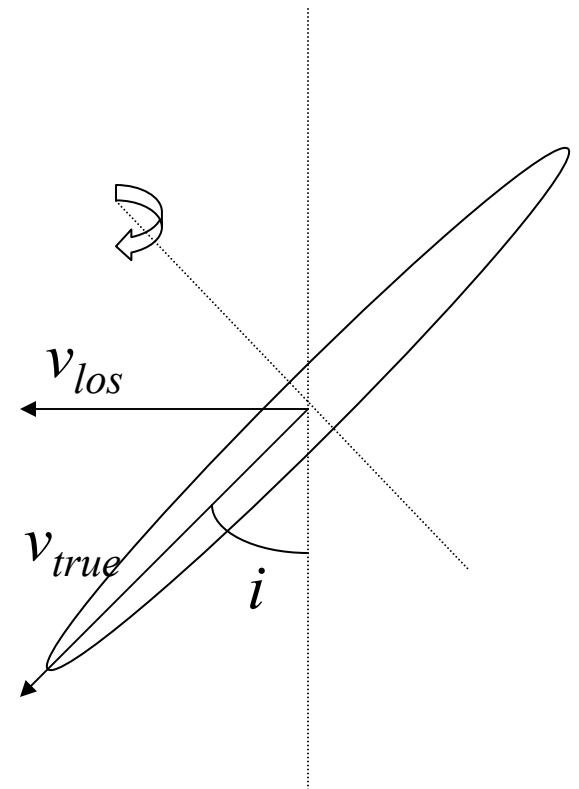
$$M_{\text{dyn}} = \frac{R \Delta v_{\text{los}}^2}{G \sin^2 i},$$

where,

- 1) Δv_{los} = line of sight velocity
- 2) R is the radius of the disk
- 3) i is the inclination angle.

Note that

$$\Delta v_{\text{true}} = \Delta v_{\text{los}} / \sin i.$$



Properties of HI & H₂ in Galaxies



- The HI extent > optical extent of galaxies ($2 - 3 R_H$ at $n = 10^{20}$ cm⁻², where R_H is the **Holmberg Radius** – the radius at which $\Sigma_{pg} = 26.5$ mags arcsec²)

- HI extent has a sharp cutoff (at $n_{HI} \sim 10^{19}$ cm⁻²)

- Many galaxies have HI holes in the central regions which correspond to the location of the stellar bulge.



(Gilmore et al., pg 203)

Distribution vs. R

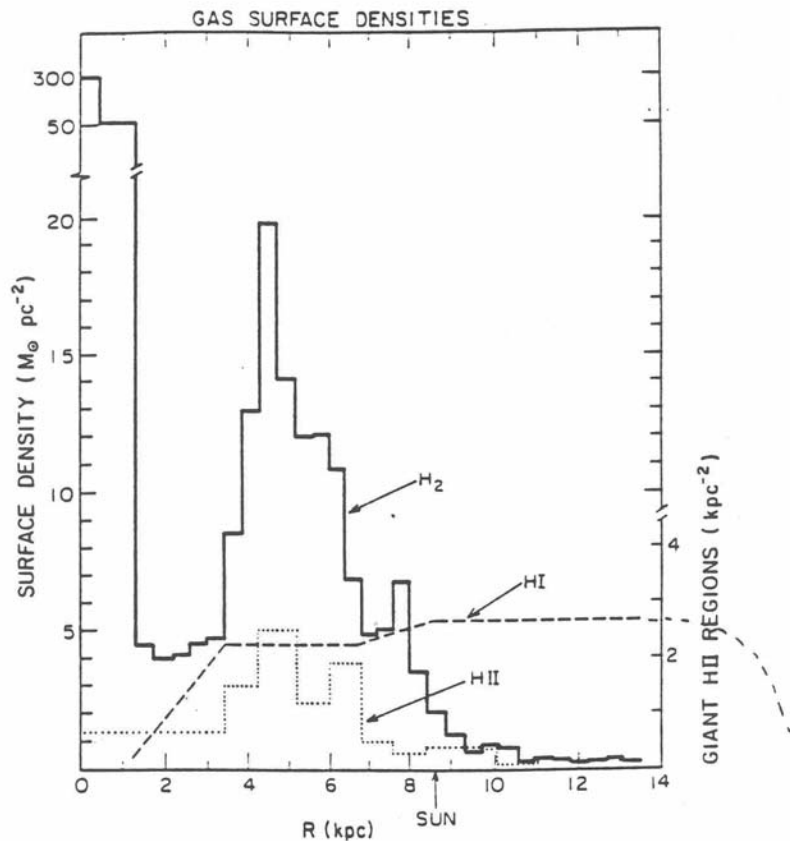


Figure 6. Comparison of gas surface densities in the Milky Way disk. Values for H_2 (Clemens, Sanders, and Scoville 1986) and HI (Burton and Gordon 1978) include a 1.36 correction factor for He and they have been scaled to $R_0=8.5$ kpc.

- HI Holes
- Some (like the Milky Way) have Molecular Rings

(Scoville & Sanders 1987, in *Interstellar Processes*, pg 21)

HI, H₂, & Dust in the Milky Way

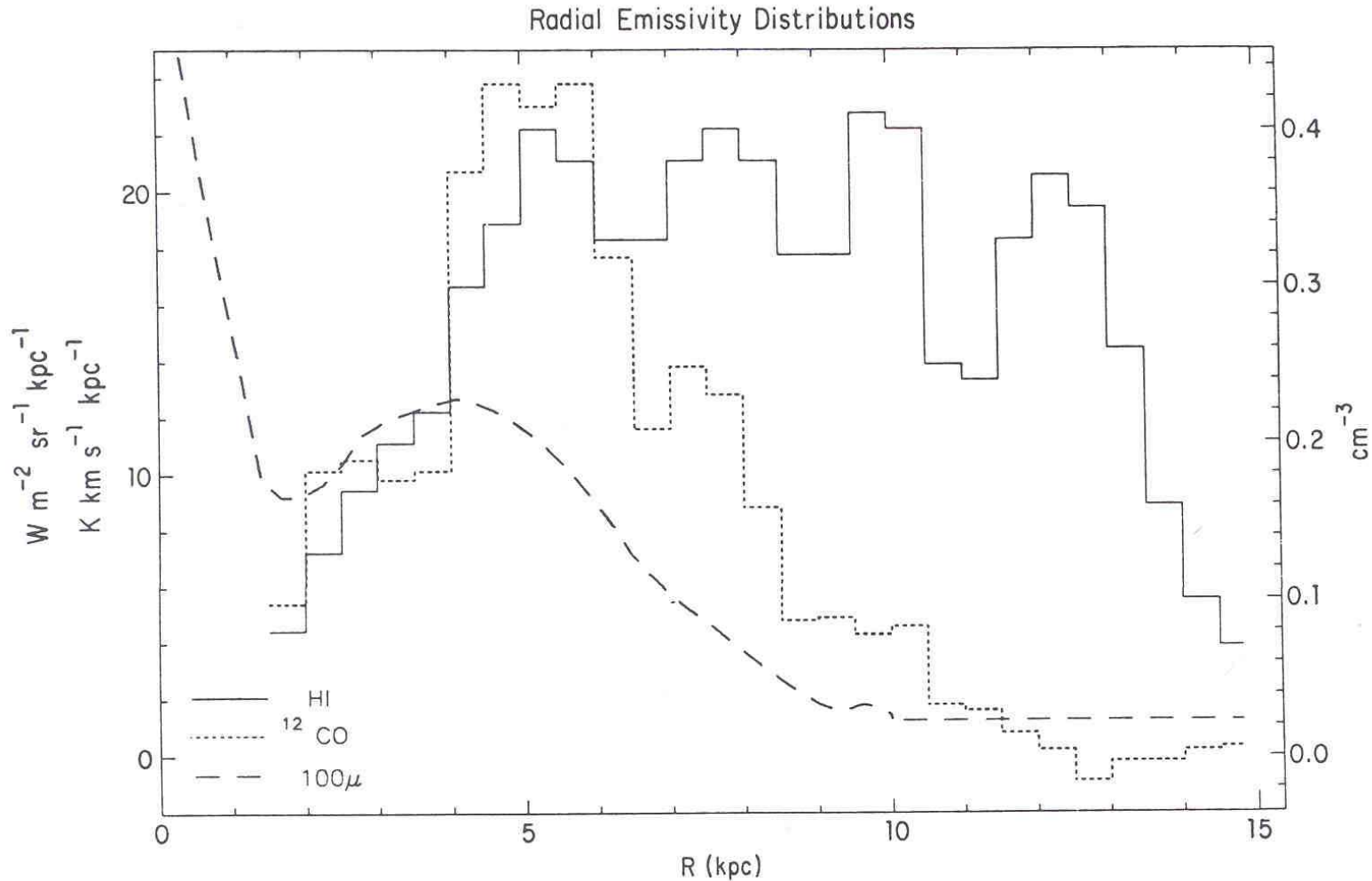


FIGURE 4.2
Radial distributions of H_I, CO, and dust. (From Burton 1988.)

(Gilmore et al., pg 68)

Counter-Example

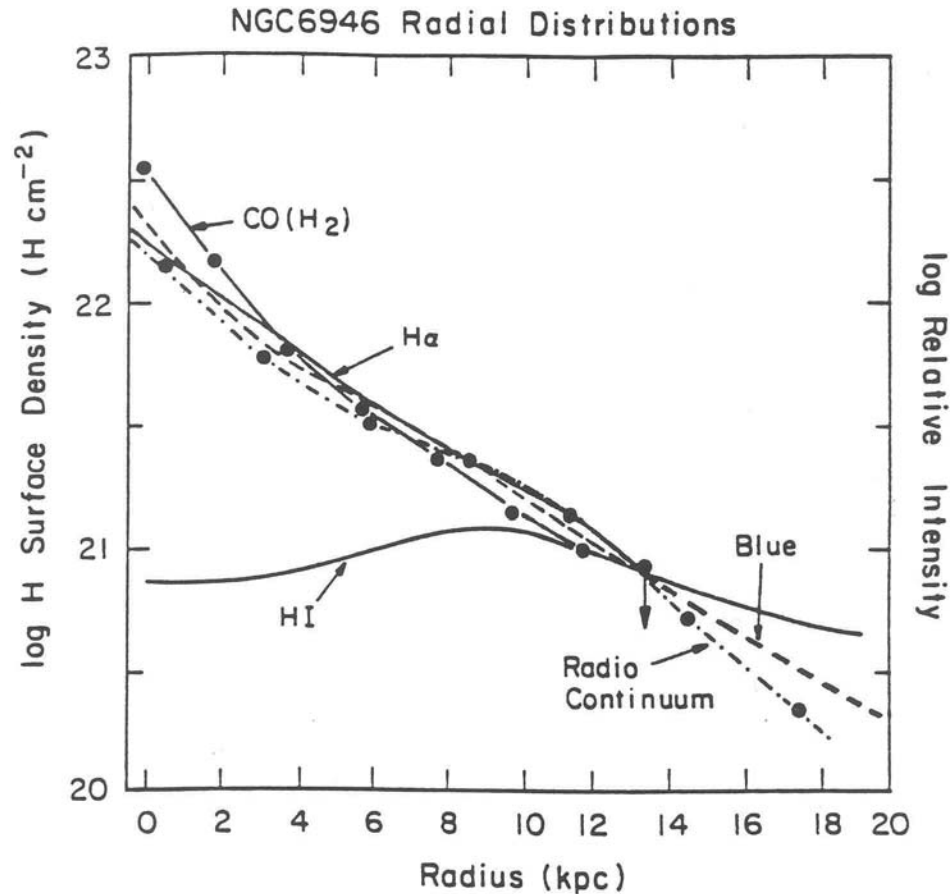
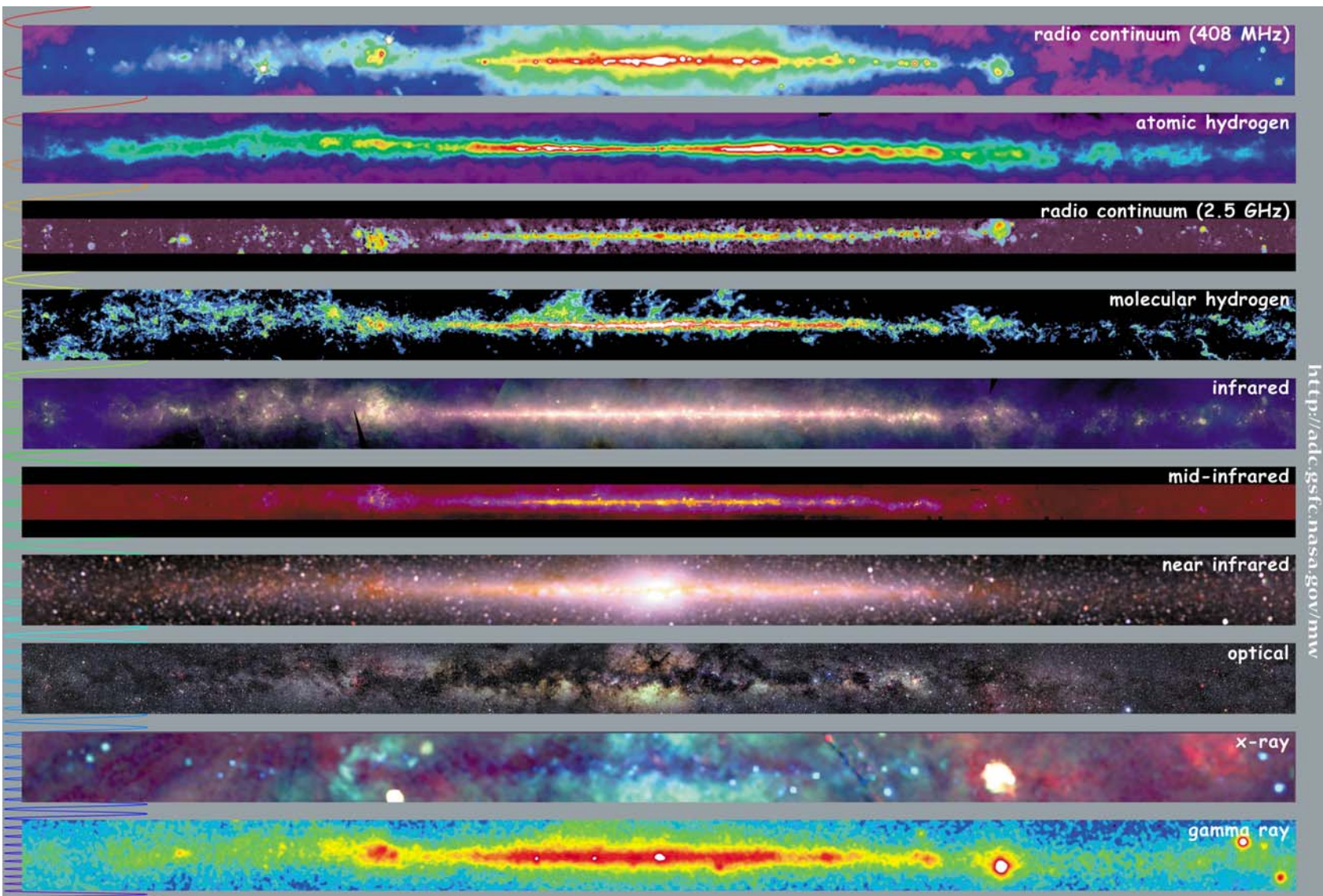


Figure 9 Comparison of the radial distributions of CO (H_2), HI, $H\alpha$, blue and radio continuum in NGC 6946 from Tacconi & Young (1986). References are given in Tacconi & Young (1986).

- No HI hole
 - No molecular ring
- (Young & Scoville 1991, ARAA, 29, 608)

Properties of HI & H₂ in Galaxies, cont.

- H₂, & not HI follows the distribution of dust & H α emission in galaxies
- This is because dust is a catalyst for H₂ formation
- and stars form in molecular clouds

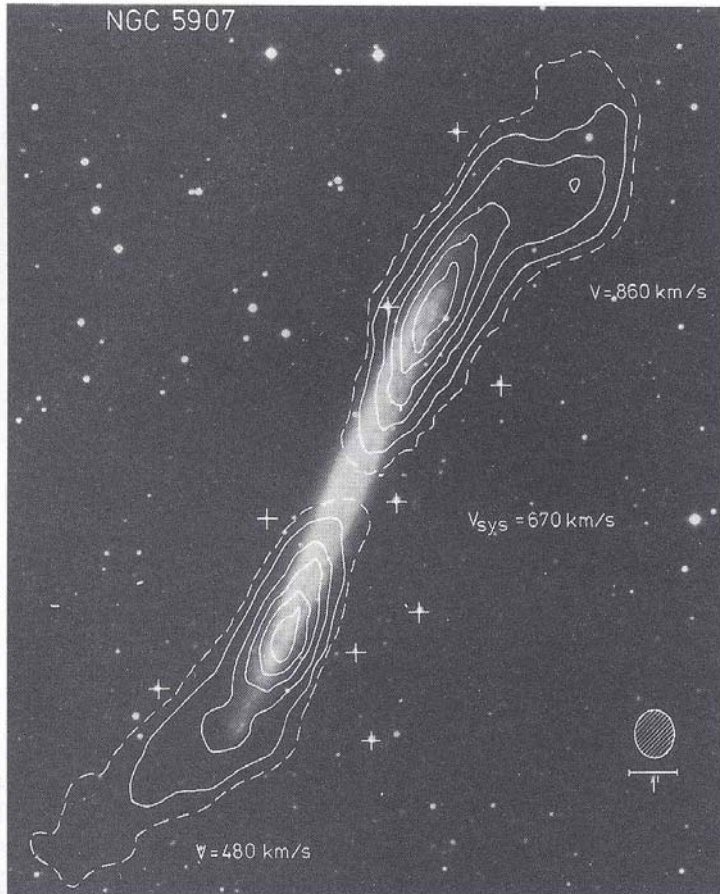


<http://adc.gsfc.nasa.gov/mw>



Multiwavelength Milky Way

HI Profile – HI Disk



- Inner part → thin (half height $\sim 500 \text{ pc}$)
- Outer part → thick & warped (i.e., beyond the optical light)

Figure 8.30 The warped neutral hydrogen disk of the nearly edge-on galaxy NGC 5907. Emission by gas that is moving near the systemic velocity of the galaxy has been suppressed for clarity. NGC 5907 has no nearby neighbors that could have recently disturbed it tidally. [After Sancisi (1976) courtesy of R. Sancisi]

(B&M pg. 504)

HI Rotation Curves

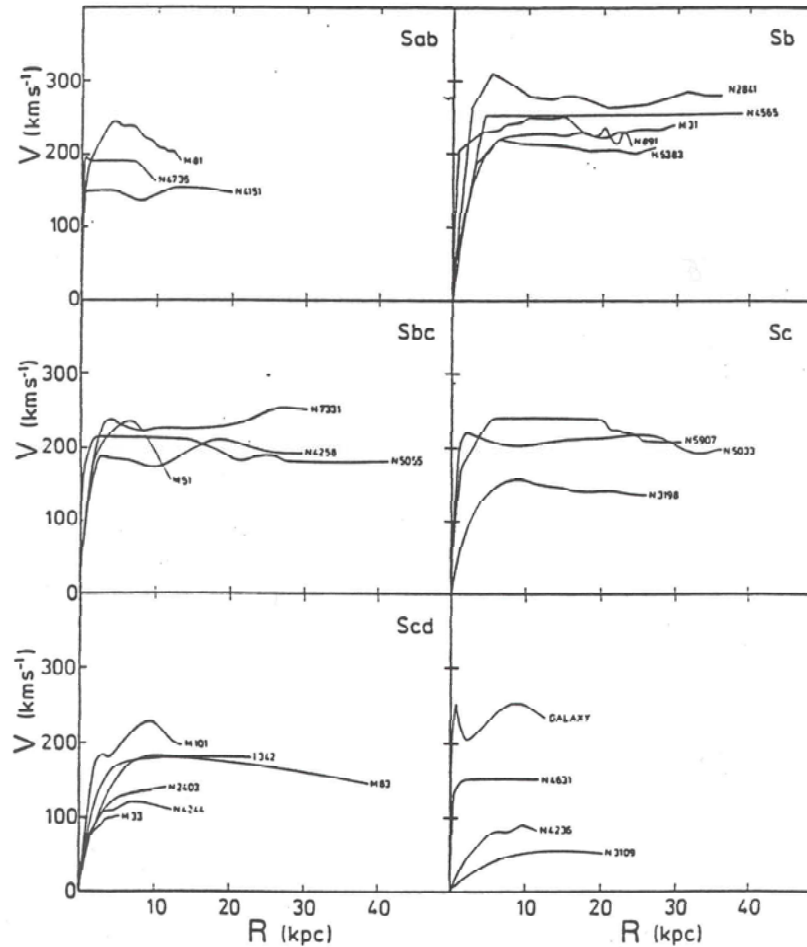


Figure 3.5 (b) HI rotation curves for several types of spiral galaxy, confirming the flatness of the optical rotation curves at far greater distances still from the centre. (From Bosma 1981.)

- Useful tracer of mass in the galaxy halo

(Galaxies & Cosmology, Combes et al., pg 71)

HI Intensity & Spider Diagrams

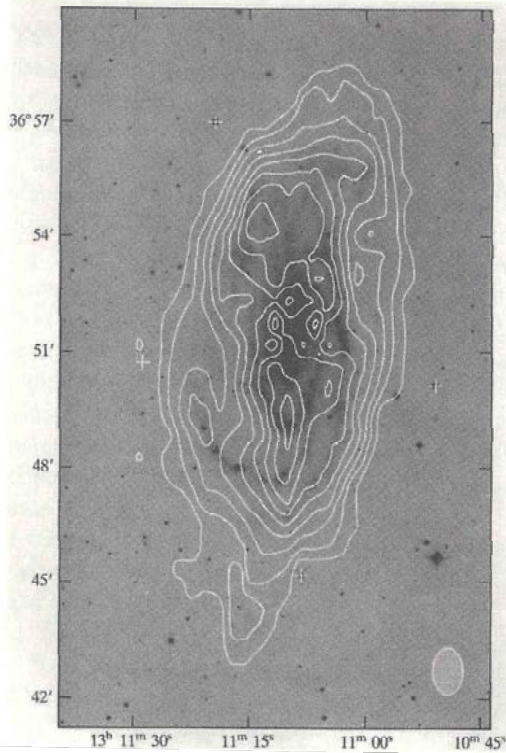


Figure 8.16 Map of the HI column density in the Sc galaxy NGC 5033 superposed on a photograph of the system. Notice that the gas appears to cover a much larger area than the optical galaxy. [After Bosma (1978)]

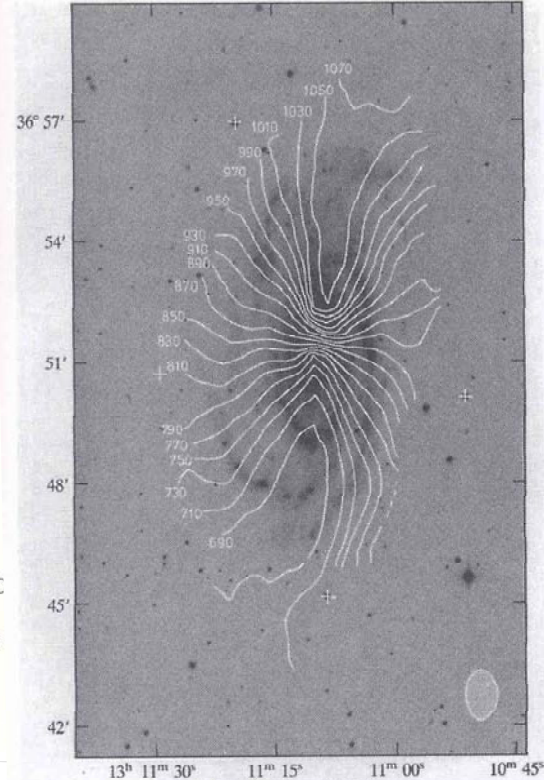


Figure 8.17 Contours of constant HI velocity in NGC 5033. Notice the curvature of the kinematic principal axes. [After Bosma (1978)]

HI Spider Diagram

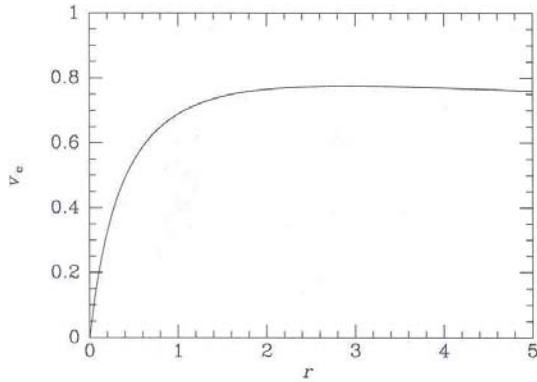


Figure 8.31 A typical galactic circular-speed curve.

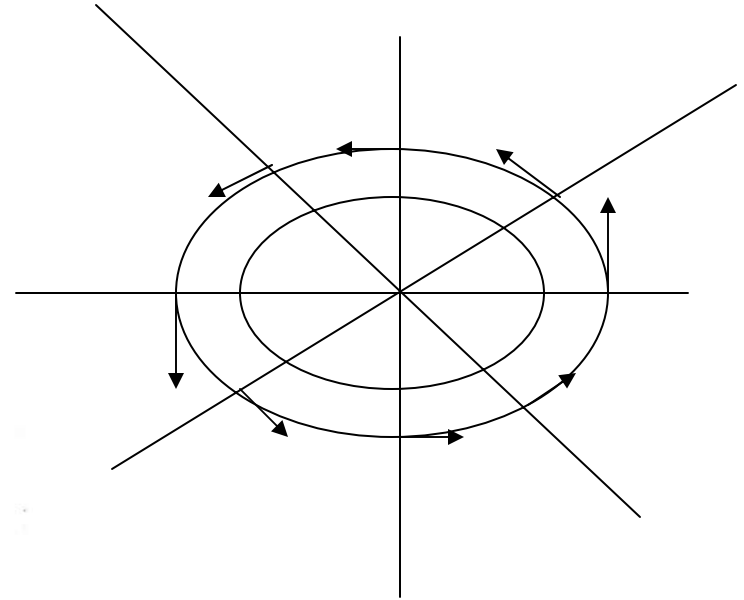
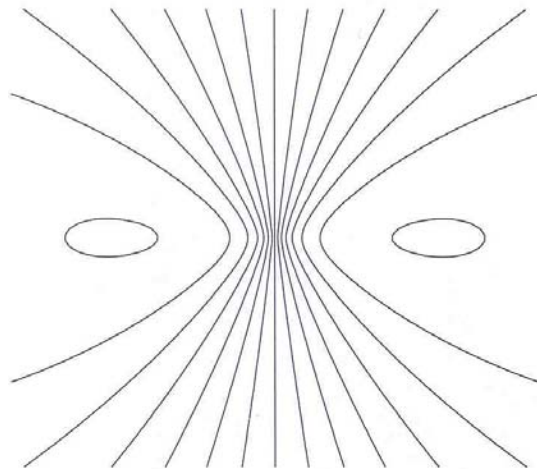
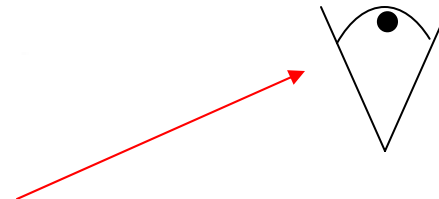


Figure 8.32 The spider diagram generated by the circular-speed curve of Figure 8.31 when the system is viewed at inclination $i = 30^\circ$ with the apparent major axis horizontal. The area contoured is a square 10 distance units on a side.



(B&M, pg 506)



The observer only sees the line of sight velocities.

Distortions in HI Spider Diagrams

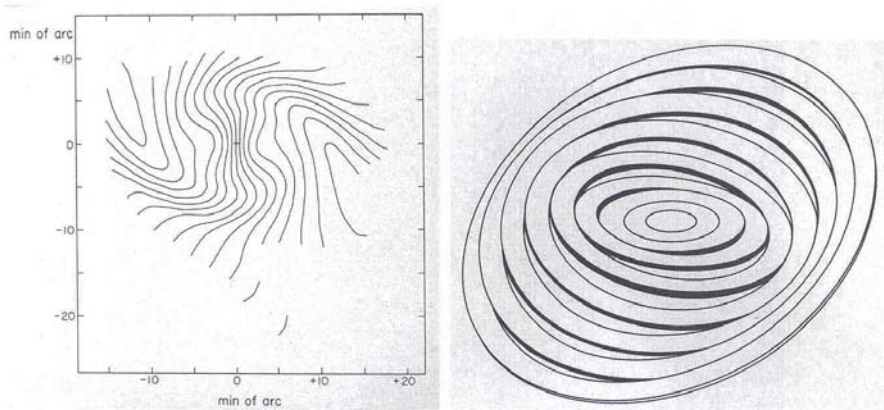


Figure 8.36 A tilted ring model of M83 (right) and the spider diagram predicted by this model (left). [After Rogstad, Lockhart & Wright (1974)]

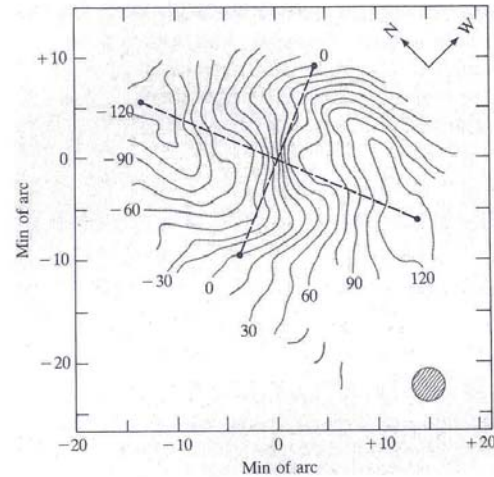


Figure 8.37 The observed spider diagram of M83. [After Rogstad, Lockhart & Wright (1974)]

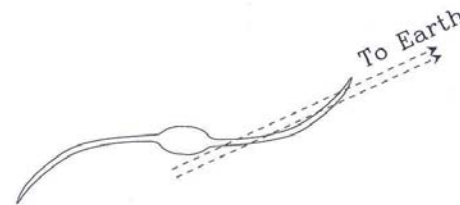
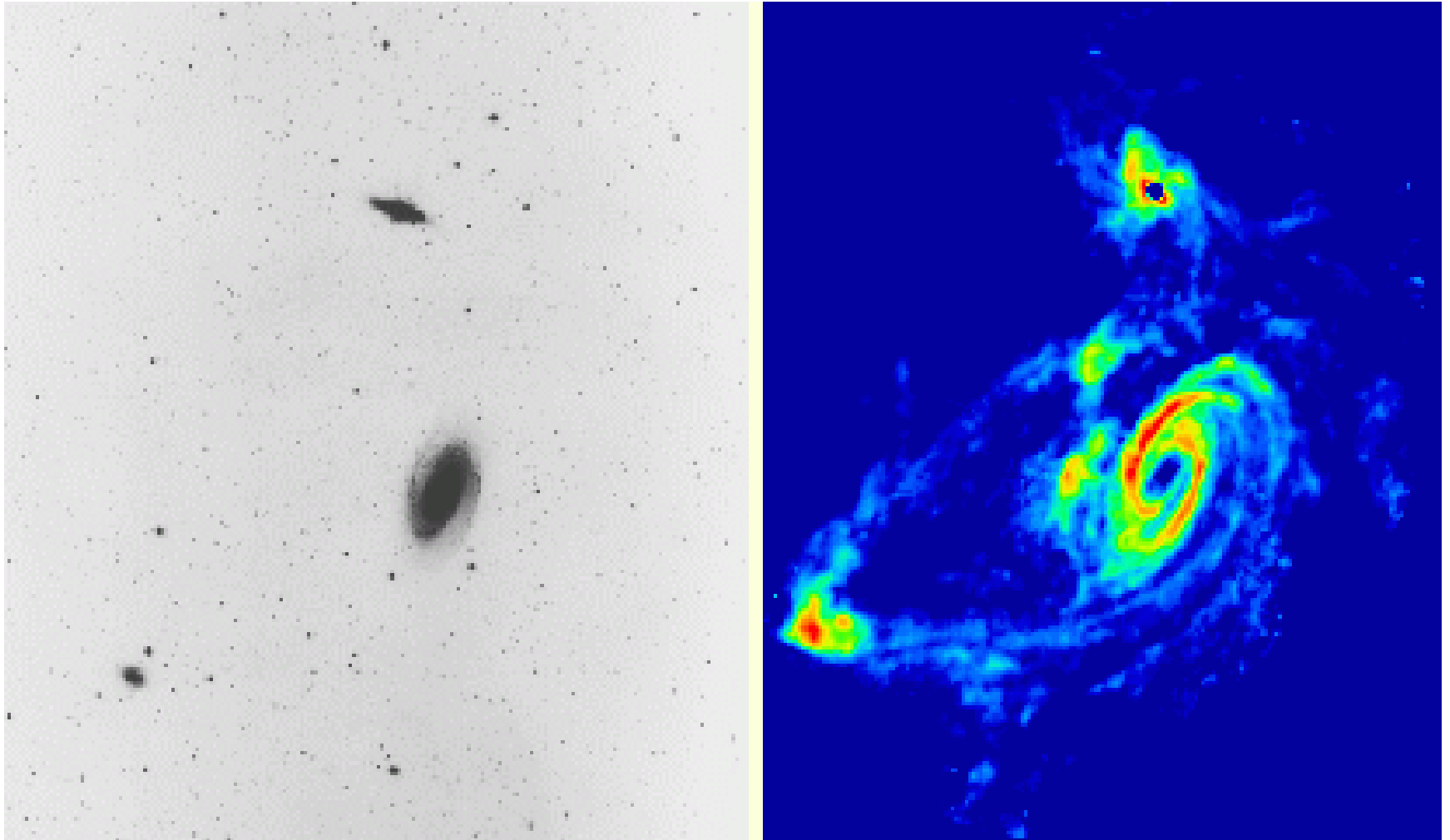


Figure 8.38 When a strongly warped disk is viewed nearly edge-on, some lines of sight cut the warped disk twice, and the line-profile is liable to be multi-peaked.

(B&M, pg 511)

HI as an Interaction Tracer



(Yun, Ho, & Lo 1993, Nature, 372, 530)

Big Picture: Finding an Elliptical Galaxy at $z \sim 2.4$ puts constraints on the age of the universe.

1994AJ.....107..1303H

TWO EXTREMELY RED GALAXIES

E. M. HU¹ AND S. E. RIDGWAY

Institute for Astronomy, University of Hawaii, 2680 Woodlawn Dr., Honolulu, Hawaii 96822

Electronic mail: hu@uhifa.ifa.hawaii.edu, ridgway@uhifa.ifa.hawaii.edu

Received 1993 September 29; revised 1993 December 20

ABSTRACT

We report the discovery of two galaxies with $(I-K) \sim 6.5$ lying near the line of sight to the $z=3.790$ quasar PC 1643+4631 A. Based on the spectral energy distributions and angular extents of the objects we suggest that the most likely interpretation is that they are elliptical galaxies lying at $z \sim 2.4$. The existence of such evolved objects at this redshift would imply a current age of the universe substantially in excess of 1.0×10^{10} yr for $q_0=0.02$, and 1.9×10^{10} yr for $q_0=0.5$. It would also imply that at least some large luminous galaxies were already fully formed at $z > 6$.

SEDs →

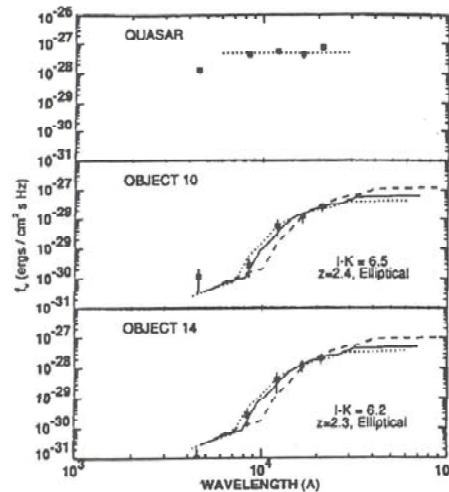


FIG. 2. Multicolor plots in B , I , J , H , and K' of the quasar and the two anomalously red objects. The quasar is well fit by a flat f_{ν} distribution above its Lyman break (dotted line). The continuum bands are substantially free of strong emission lines at the quasar redshift over these colors, with some slight contamination at the edge of the K' band from $H\beta$. In contrast, the ultrared objects show strong color drops between K and I . Using an elliptical SED (from Coleman *et al.* 1980) to characterize the light distribution, we obtain the best fit for a redshift of $z \sim 2.4$, where $(I-K)$ is maximized. The range in elliptical SED redshift fits from $z=1.8$ (dotted) to $z=3$ (dashed) is shown bracketing the best fit redshift values.

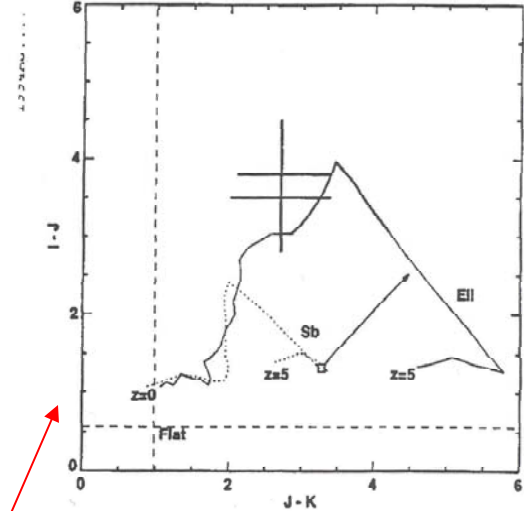


FIG. 4. Color-color plots showing constraints of $(I-J)$ colors. Measured colors in $(I-J)$ and $(J-K)$ of the two ultrared objects are shown with heavy (overlapping) crosses. Colors of Sb (dotted) and elliptical (solid) galaxies are shown as a function of redshift, from blue ($z=0$) to red ($z=5$) values. The heavy solid line shows the color range of $z=2-3$ ellipticals, with the reddest $(I-J)$ values for $z=2.4$. Color values for flat $(I-J)$ and flat $(J-K)$ objects are shown with dashed lines, and flat spectrum objects should have colors near the intersection of these curves. The arrow shows the effect of reddening on the measured colors using the colors of an Sb with $3 < z < 4$ as an origin. The intrinsic $J-K$ colors of an Sb in this redshift range (e.g., coincident with the quasar's redshift [$z=3.790$] or that of the candidate damped absorption system [$z=3.14$]) are already too high for reddening to produce an adequate fit to the observed colors of the ultrared objects.

Color-color diagram with redshifted elliptical galaxy model

THE REDSHIFT OF AN EXTREMELY RED OBJECT AND THE NATURE OF THE VERY RED GALAXY POPULATION¹

JAMES R. GRAHAM

Astronomy Department, University of California, Berkeley, Berkeley, CA 94720; jrg@graham.berkeley.edu

AND

ARJUN DEY

KPNO/NOAO, ²950 North Cherry Avenue, P.O. Box 26732, Tucson, AZ 85726; dey@noao.edu

Received 1996 January 26; accepted 1996 June 12

ABSTRACT

Infrared surveys have discovered a significant population of bright ($K \lesssim 19$) extremely red ($R - K \gtrsim 6$) objects. Little is known about the properties of these objects on account of their optical faintness ($R \gtrsim 24$). Here we report deep infrared imaging and spectroscopy of one of the extremely red objects (EROs) discovered by Hu & Ridgway in the field of the $z = 3.79$ quasar PC 1643+4631A. The infrared images were obtained in 0".5 seeing and show that the object (denoted HR 10) is not a dynamically relaxed elliptical galaxy dominated by an old stellar population as was previously suspected, but instead has an asymmetric morphology suggestive of either a disk or an interacting system. The infrared spectrum of HR 10 shows a single, possibly broad emission feature at $1.60 \mu\text{m}$, which we identify as $\text{H}\alpha + [\text{N II}]$ at $z = 1.44$. The luminosity and width of this emission line indicates either intense star formation ($\sim 20 h^{-2} M_{\odot} \text{yr}^{-1}$) or the presence of an active nucleus. Based on the rest frame UV-optical spectral energy distribution, the luminosity of HR 10 is estimated to be $3-8 L^{\odot}$. The colors of HR 10 are unusually red for a galaxy (at $z = 1.44$ the age of HR 10 is at most 2-8 Gyr depending on cosmology) and indicate that HR 10 is dusty. HR 10 is detected weakly at radio wavelengths; this is consistent with either the starburst or active galactic nucleus hypothesis. If HR 10 is a typical representative of its class, EROs are numerous and represent a significant component of the luminous objects in the universe at $z \approx 1.5$.

Subject headings: galaxies: evolution — galaxies: photometry — galaxies: stellar content — galaxies: structure — infrared: galaxies

- Images of HR 10: very asymmetric
- **Conclusion:** HR 10 cannot be a dynamically relaxed system (i.e., like an elliptical galaxy)

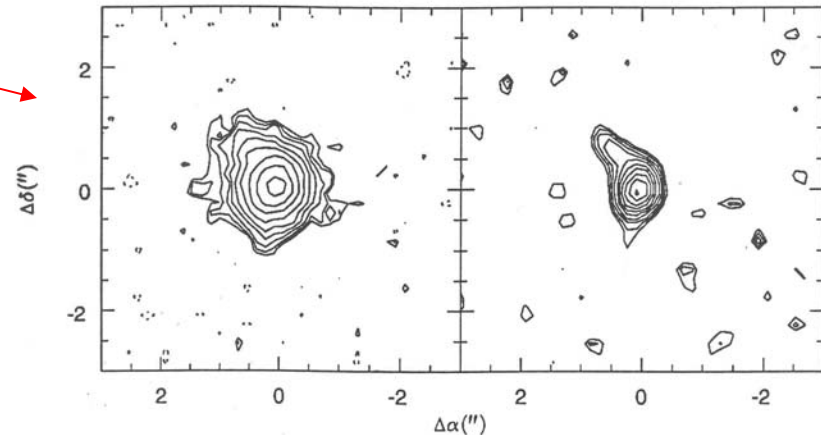


FIG. 2.—(a) Contour plot of the Keck K-band image of HR 10 showing the asymmetric structure to the northeast of the galaxy. The solid contours are drawn at levels $(2, 3, 4, 5, 6, 7, 8, 9, 10) \times \sigma_{\text{sky}}$, where $\sigma_{\text{sky}} = 22.28 \text{ mag arcsec}^{-2}$. The dotted line represents the $-2\sigma_{\text{sky}}$ contour level. (b) Lucy deconvolution of the K-band image using a point-spread function constructed from the QSO PC 1643+4631A. The contour levels are drawn as in (a), but with σ_{sky} equivalent to $21.38 \text{ mag arcsec}^{-2}$. The deconvolved image has a resolution FWHM of ≈ 0.728 .

H α + [N II] Confirms redshift of $z = 1.44$

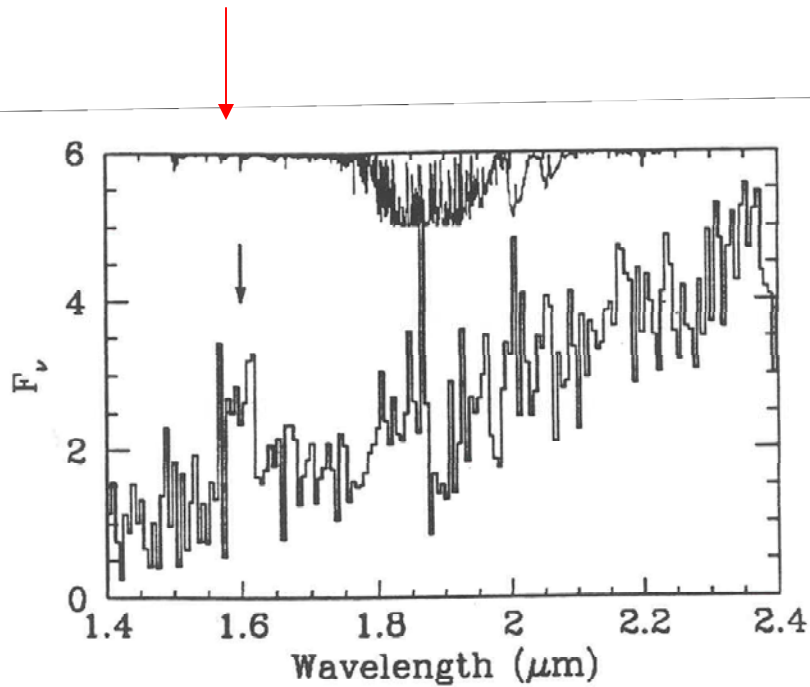


FIG. 3.—Keck IR spectrum of HR 10 showing a broad emission feature at 1.6 μm (indicated by the arrow). The most likely identification for the emission feature is H α + [N II] at $z \approx 1.44$. The ordinate is in relative F_ν units. The atmospheric transmission spectrum extracted from the National Solar Observatory IR Solar Atlas (Livingston & Wallace 1991) is shown as the light line at the top of the plot. The atmospheric curve has been shifted such that the transmission is unity at the top of the plot, and zero where the ordinate has a value of 5.

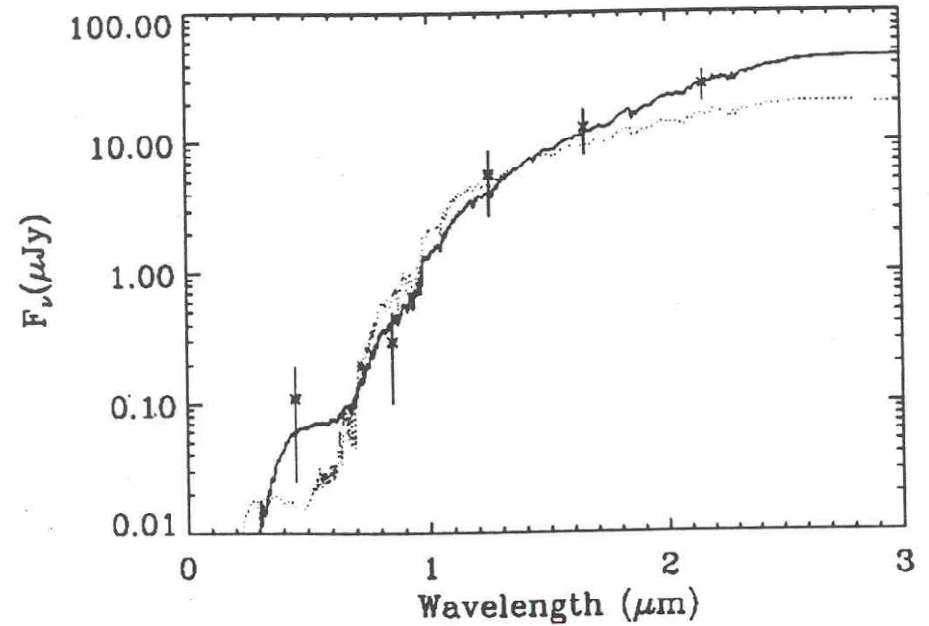


FIG. 4.—Broadband photometry of HR 10 compared with the best-fit model Sbc galaxy SED (solid line) at $z = 1.44$ ($A_V = 1.8$). The dotted line is the best-fit unreddened elliptical galaxy SED at $z = 1.44$.

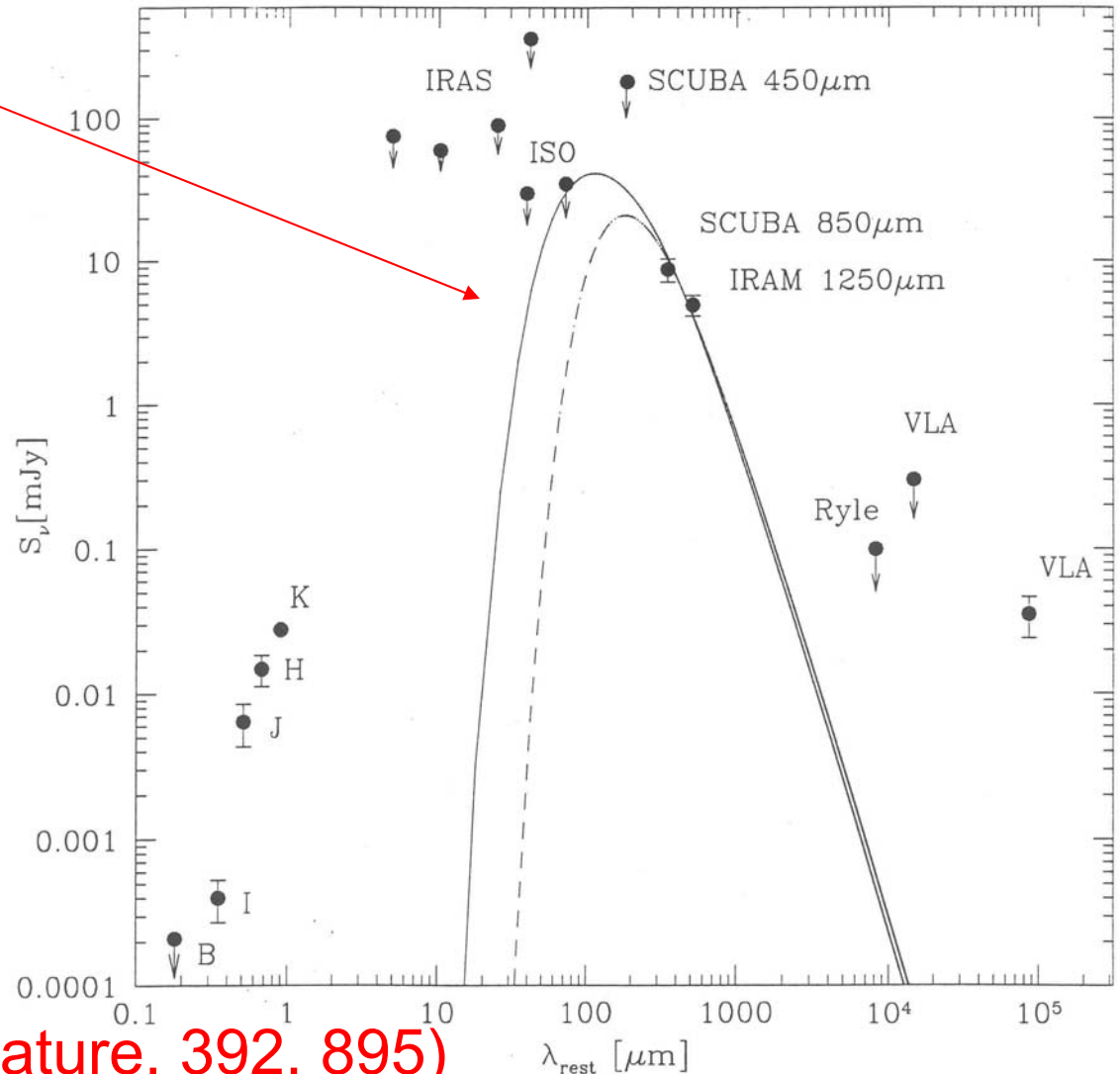
(Graham & Dey)

SED of HR10 plus model of
a $z=1.44$ Sbc Spiral Galaxy.

Vigorous star formation hidden by dust in a galaxy at $z = 1.4$

Andrea Cimatti¹, Paola Andreani²,
Huub Röttgering³, Remo Tilanus^{4,5}

- Very dusty
- Where there's dust, there's H_2



(Cimatti et al. 1998, Nature, 392, 895)

CO detection of the extremely red galaxy HR10

Paola Andreani¹, Andrea Cimatti², Laurent Loinard³, and Huub Röttgering⁴

¹ Osservatorio Astronomico di Padova vicolo dell'Osservatorio 5, I-35122 Padova, Italy, e-mail: andreani@pd.astro.it

Present-address: Max-Planck I. f. extraterrestrische Physik, Postfach 1603, D-85740 Garching, Germany

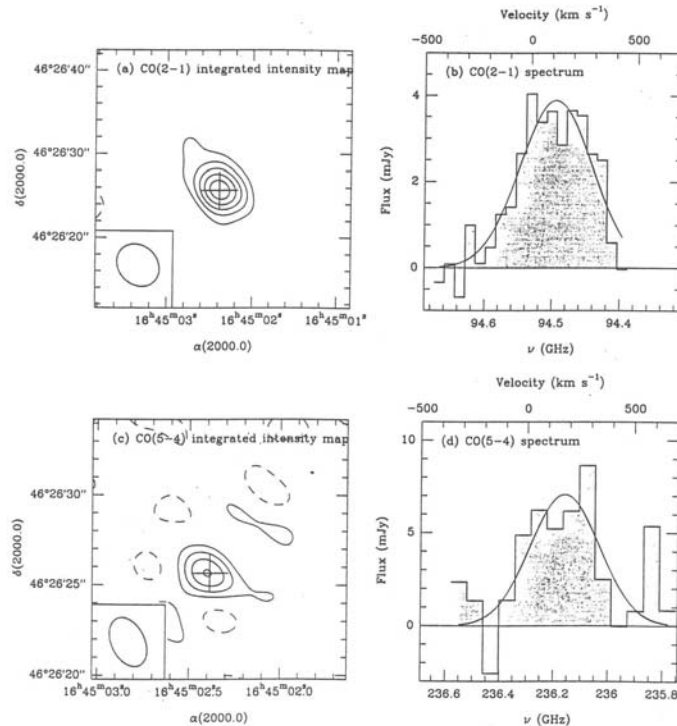
² Osservatorio Astrofisico di Arcetri, Largo E. Fermi 5, I-50125 Firenze, Italy, e-mail: cimatti@arcetri.astro.it

³ Institut de Radioastronomie Millimétrique, 300, rue de la Piscine, St. Martin d'Hères, France e-mail: loinard@iram.fr

⁴ Sterrewacht Leiden, Sterrewacht, Postbus 9513, Leiden 2300 RA the Netherlands e-mail: rottgeri@strw.leidenuniv.nl

Abstract. CO $J = 5 - 4$ and $J = 2 - 1$ emission lines were detected towards the extremely red galaxy (ERG) HR10 (J164502+4626.4) at $z = 1.44$. The CO intensities imply a molecular gas mass $M(\text{H}_2)$ of $1.6 \times 10^{11} h_{50}^2 M_{\odot}$, and, combined with the intensity of the dust continuum, a gas-to-dust mass ratio around 200-400 (assuming galactic values for the conversion factors). The peak of the CO lines are at the same redshift as the [OIII]3272 line, but

blue-shifted by 430 km s^{-1} from the $\text{H}\alpha$ line. These CO detections confirm the previous results that HR10 is a highly obscured object with a large thermal far-infrared luminosity and a high star-formation rate. The overall properties of HR10 (CO detection, L_{FIR} to L'_{CO} ratio, and FIR to radio flux ratio) clearly favour the hypothesis that its extreme characteristics are related to star-formation processes rather than to a hidden AGN.



CO Transitions

Fig. 1. (a) CO(2-1) integrated intensity map; the contours are at $0.25 \text{ Jy beam}^{-1} \text{ km s}^{-1}$. (b) CO(2-1) spectrum at the center of the source. (c) CO(5-4) integrated intensity map; the contours are at $0.75 \text{ Jy beam}^{-1} \text{ km s}^{-1}$. (d) CO(5-4) spectrum at the center of the source. The contribution from the continuum is not subtracted from the line

(Andreani et al. 2000, A&A, 354, 1)